Study and Simulation of Helicopter Gearboxes Noise

Guillaume Roulois, Franck Marrot, Julien Caillet, Alexandre Loredo, Thomas Dupont

Paper number 102

STUDY AND SIMULATION OF HELICOPTER GEARBOXES NOISE

Guillaume Roulois[1,2,3], Franck Marrot[1], Julien Caillet[1], Alexandre Loredo[2], Thomas Dupont[2]

[1]*EUROCOPTER,* ETGV – Dynamics Department, *13725 Marignane Cedex France*
[2]*Université de Bourgogne, LRMA-Nevers, ISAT, 49 rue Mlle Bourgeois, 58027 Nevers, France*
[3]*Corresponding author: guillaume.roulois@eurocopter.com*

ABSTRACT

Main gearbox is one of the main noise sources in helicopter cabin. In order to improve the comfort of customers and reduce the health impact, acoustic and vibration mechanisms of gearboxes have to be understood and simulated during development phases. Thus, we first present the global methodology chosen to compute main gearboxes noise in helicopter cabins. Secondly, we described the way we compute mechanical excitation sources induced from gear mesh, static transmission error and meshing stiffness. Depending on the type of gear, we compute those using either analytical specially developed code or EC codes. Thirdly, we propose a modeling to compute dynamic loads on bearings being the excitation sources for the housing. We propose to compute them in the case of transmissions composed of several cylindrical and/or spiral bevel gear pairs. This modeling relies on a finite element method generally used in the case of overall acoustic and vibration studies of rotating machines. At last, a realistic example is proposed and some conclusions are drawn concerning the capability of this model.

Keywords: gear noise, cylindrical gear, spiral bevel gear, bearing loads, transmission error, meshing stiffness, helicopter internal noise

1. INTRODUCTION

Nowadays, means of transport have to be as quiet as possible regarding internal noise level in order to improve the comfort of customers and reduce the health impact. The improvement of acoustic comfort in helicopter cabins has been a priority of Eurocopter (EC) for several years. In this context, several development axes have been identified by the company. Among them, one is dedicated to the reduction of helicopter main gearboxes (MGB) noise. The latter has been identified as one of the main noise sources in helicopter cabins [1], and psychoacoustical studies have proved that it penalizes acoustic comfort of crew and above all passengers. Indeed, MGB noise perceived within helicopter cabins is a sum of tones located in the frequency range where human ear is the most sensitive. These noises are generated by the gear meshing phenomena of MGB gear trains. They are harmonics of gear mesh frequencies and their noise level could be up to +30dB higher than broad band noise. Figure 1 shows the main noise sources perceived in helicopter cabins. Figure 2 shows the noise spectrum measured in a helicopter cabin and main noise sources are identified.

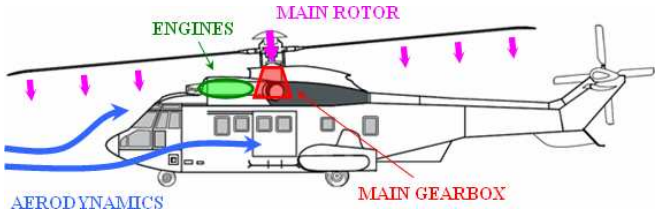

Figure 1: Main noise sources in helicopter cabins

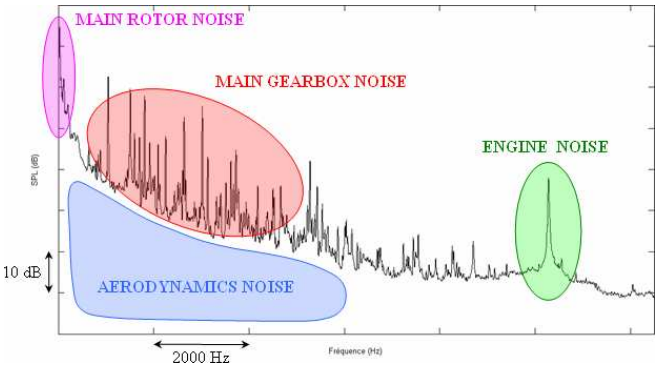

Figure 2: Noise spectrum measured in helicopter cabins

In order to reduce the impact of MGB noise, vibro-acoustic mechanisms of gearboxes have to be understood and modeled during the development phases. By this way, MGB noise and vibration sources could be identified and the vibro-acoustic behavior could be improved through an appropriate design, thus reducing cost, additional weight and integration difficulties of sound-proofing solutions.

This paper presents the current EC/LRMA developments regarding the modeling of gearboxes dynamic behavior for MGB noise computation. In the context of industrial applications, the target is to develop a simple tool for fast calculations thus allowing to conduct several parametric studies and to tune the gearboxes design in early development phases.

2. METHODOLOGY FOR COMPUTATION OF GEARBOXES NOISE

Gearboxes noise and vibration simulation is a complex problem that can be split into three major consecutive computation steps [6] [8] [9]. Nevertheless, each step can be used separately to perform parametric studies. The final goal of the model is to be able, for given operating conditions including torque and rotational speed, to predict the noise generated for any MGB design configuration. According to bibliography, we consider mechanical excitation sources induced from gear mesh phenomena as being the main causes of noise radiated from operating gearboxes.

The first step of the chosen methodology computes static transmission error and meshing stiffness of gear pairs under quasi-static load. These parameters have been identified for many years as the dominant mechanical excitation sources of gear drive trains [2] [3] [4] [5]. They mainly depend on gears geometry, operating load and manufacturing defects, and describe the elastic coupling between meshed gears. These parameters can be used as an input to compute dynamic response of drive train.

The second step consists in computing drive train modes and dynamic response including the modeling of all its components (gear bodies, drive shafts and elastic bearings). The target is to determine the dynamic loads applied on bearings for given gear mesh excitation, these loads being the main excitation sources of the gearbox housing [7].

At last, these dynamics loads are the input data to perform the computation of the overall vibro-acoustic behavior. It is based on the use of a Boundary Element Method of a commercial tool. This is the third step of the proposed methodology.

In the case of helicopter applications, a fourth step is dedicated to studying of noise and vibrations transfer paths from MGB to inside the cabin. Indeed, helicopter MGB is located above the cabin and fixed to the fuselage in several spots. The fixing system of MGB onto the structure carries all the flight loads (main rotor torque and lift loads). Thus, MGB noise within helicopter cabins is the result of two contributions. The first one is an airborne contribution. This is the part of MGB noise transmitted inside the cabin through the structure. The second one is a structural borne contribution. MGB vibrations are transmitted through the fixing system to the structure which radiates under their effects. Figure 3 illustrates the computation steps of the methodology proposed to study helicopter MGB noise.

In this paper, we describe the current EC/LRMA developments regarding the steps 1 and 2. Step 3 will be tackle during the coming months using a commercial tool to compute overall vibro-acoustic of a helicopter gearbox. Step 4 has been studied in EC for several years but it isn't included in this document.

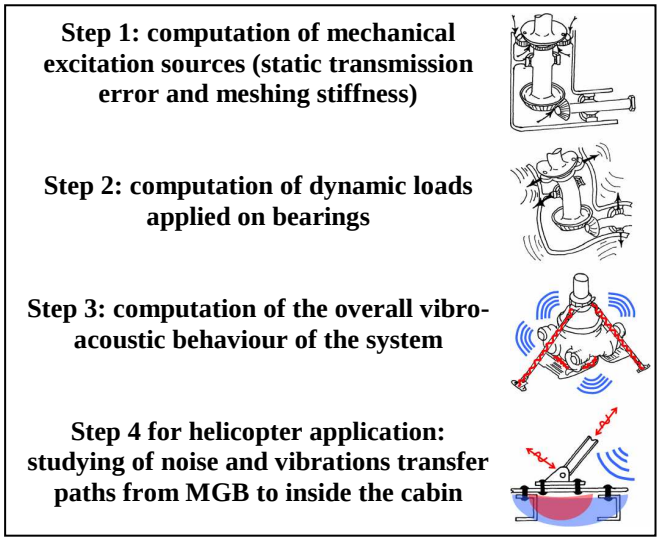

Figure 3: Methodology for computation of MGB noise

3. STATIC TRANSMISSION ERROR AND MESHING STIFFNESS

3.1. STATIC TRANSMISSION ERROR

Static transmission error (STE) is defined as the difference between the actual position of the output gear and the position it would occupy if the gear drive were geometrically perfect and infinitely rigid [5]. STE is computed under a steady torque for each position of the input pinion by solving the static–elastic balance of the gear contact problem. This quasi-static parameter depends on manufacturing defects and elastic deformations of meshed teeth under load (bending and contact crushing), and it isn't linear with load. STE has been identified as the dominant mechanical excitation sources of gear drive trains. It is strongly correlated with gear noise in magnitude and spectral content [2] [3] [4] [5]. Figure 4 defines STE of cylindrical gears [10].

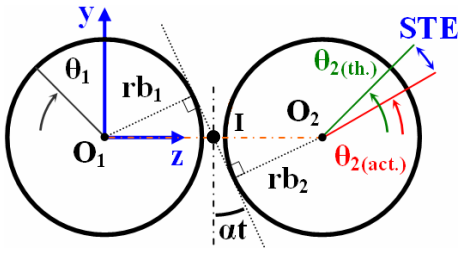

Figure 4: STE of cylindrical gears (angular expression)

In the case of cylindrical gears (Figure 4), STE is defined at the pitch point I as follows:

$$STE(T,\theta_1)_{[rad]} = \theta_2^{THEORETICAL}(\theta_1) - \theta_2^{ACTUAL}(T,\theta_1)$$
$$STE(T,\theta_1)_{[rad]} = \theta_1 \cdot \frac{rb_1}{rb_2} - \theta_2^{ACTUAL}(T,\theta_1) \quad (1)$$

$i = 1$, input cylindrical pinion. $i = 2$, output cylind. wheel.

rb_i is the base radius of gear i [m].

θ_i is the angular position of gear i [rad].

T is the operating input torque [N.m].

By definition, STE is an angular position [rad] but it is more often expressed as a linear displacement [m]. This linearized formulation is highly practical for computing meshing stiffness described later in this paper (3.2). In the case of cylindrical gears, STE has often been defined as a displacement along the theoretical line of action [10] and (1) becomes:

$$STE(T,\theta_1)_{[m]} = rb_1 \cdot \theta_1 - rb_2 \cdot \theta_2^{ACTUAL}(T,\theta_1) \qquad (2)$$

In the case of bevel gears, STE is defined at the mean point M (Figure 8) as follows [11]:

$$\begin{aligned} STE(T,\theta_1)_{[rad]} &= \theta_1 \cdot \frac{rm_1}{rm_2} - \theta_2^{ACTUAL}(T,\theta_1) \\ STE(T,\theta_1)_{[m]} &= rm_1 \cdot \theta_1 - rm_2 \cdot \theta_2^{ACTUAL}(T,\theta_1) \end{aligned} \qquad (3)$$

i = 1, input bevel pinion. *i = 2*, output bevel wheel.

rm_i is the mean radius of gear *i* [m].

Computing STE can be a complex problem for some kinds of gears.

Concerning cylindrical spur gears, STE can be estimated with an analytical modeling taking into account teeth geometry, operating input torque and material properties. The idea is to simulate one single meshed teeth pair over the whole path of contact. These teeth are considered as being plane beams clamped on the foot cylinder of each gear. For each successive position of the input pinion, theoretical point of contact and loads are computed and located on the beams. Thus, bending and contact crushing are computed for each of them then converted into STE depending on angular position of the pinion.

In the case of cylindrical helical gears and spiral bevel gears, STE can't be estimated with the simple approach described above. Indeed, these problems have to be processed in space using finite elements. In order to design gears during development phases of MGB, Eurocopter engineers use two softwares. These softwares simulate the quasi-static behavior of loaded gears with corrected profiles or not. First one simulates cylindrical gears with spur or helical teeth. Planetary gears are composed of cylindrical gears and they are simulated with this code. Second one simulates spiral bevel gears with Gleason teeth. Both of them compute $STE(T,\theta_1)_{[rad]}$ and several other parameters. We propose to use STE computed with these Eurocopter softwares to estimate meshing stiffness described below.

3.2. MESHING STIFFNESS

Meshing stiffness characterizes the elastic coupling between meshed gears induced from STE and operating torque. Thus, as STE, meshing stiffness is a periodic function at the gear mesh frequency depending on both operating input torque and angular position of gears. It is modeled as an oriented spring and is essential for the overall dynamic modeling of the transmission described later in this paper. Figure 5 illustrates meshing stiffness in the case of cylindrical gears.

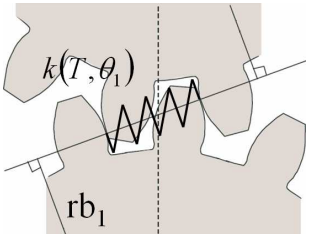

Figure 5: Illustration of meshing stiffness

Meshing stiffness isn't linear with the load. In the case of cylindrical gears, meshing stiffness is defined at the pitch point I as follows [18]:

$$k(T,\theta_1) = \frac{\partial T}{rb_1 \cdot \partial\left(STE(T,\theta_1)_{[m]}\right)} \qquad (4)$$

In other words, this means that computing meshing stiffness of a gear pair for a given operating input torque requires at least two computations of STE around this operating torque:

$$k(T,\theta_1) = \frac{T+\Delta T}{rb_1 \cdot \partial\left(STE(T+\Delta T,\theta_1)_{[m]}\right)} - \frac{T-\Delta T}{rb_1 \cdot \partial\left(STE(T-\Delta T,\theta_1)_{[m]}\right)} \qquad (5)$$

In the case of bevel gears, we propose to define meshing stiffness at the mean point M using (3) and (4):

$$k(T,\theta_1) = \frac{\partial T}{rm_1 \cdot \partial\left(STE(T,\theta_1)_{[m]}\right)} \qquad (6)$$

Once $k(T,\theta_1)$ were computed, θ_1 [rad] has to be converted into time [s] using operating rotation speed of the input pinion [rad.s^{-1}]. Thus, $k(T,\theta_1)$ becomes $k(T,t)$ and an excitation source in the dynamic modeling of the transmission described below.

4. DYNAMIC MODELING OF GEARBOXES

4.1. INTRODUCTION

In order to predict the noise generated by a gearbox, a dynamic modeling of the whole drive train with operating conditions has to be done. The goal of this step is to compute the dynamic response of the operating system to STE and meshing stiffness excitations. In particular, we need to compute the dynamic loads on bearings. These ones excite mechanically the gearbox housing which radiates under their effects. This radiation has been proved as being the main noise source of an operating gearbox [7].

4.2. OVERALL MODELING OF DRIVE TRAIN

The approach chosen to compute drive train dynamic response relies on an existing finite element matrixial method generally used in the case of overall acoustic and vibration studies of rotating machines. This approach considers a linear mesh interface and the modeling of a gear pair with shafts and elastic bearings in the local frame of meshed teeth [12] [18]. The model includes torsion, bending and longitudinal motions of drive shafts. For helicopter applications, we propose to extend the model

to two or more cylindrical and/or bevel gear pairs where degrees of freedom (DoF) are expressed in a global frame associated to the gearbox housing. Shear and gyroscopic effects on the dynamic behavior of shafts can be included in the modeling. Moreover, regarding EC needs, we choose to model and solve this dynamic step with stand-alone MATLAB functions we have programmed.

In this program, shafts are discretized with three-dimensional beam elements. Each element is composed of two nodes with six DoF per node expressed in the global frame of the housing. Each beam element is characterized by three [12x12] matrixes: stiffness, mass and damping. The terms of these elementary matrixes are perfectly known. For helicopter applications, they rely on Timoshenko formulation taking into account shear effects which have a significant impact on the bending behavior of short shafts. Moreover, elementary matrixes that we use take into account gyroscopic effects which also modify bending behavior of shafts operating with high rotation speed. These matrixes are referenced in [13] [14] [15] [16] [17]. They are computed using material and geometrical properties of the consecutive sections of the shaft. Figure 6 shows discretization of an existing MGB shaft using 17 successive beam elements (18 nodes). This shaft is carried by two bearings at nodes 2 and 17.

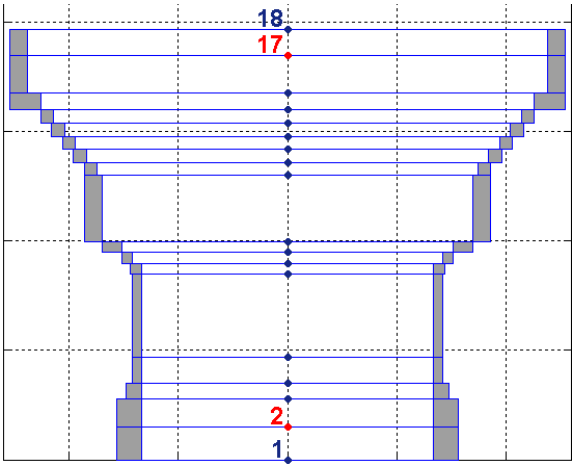

Figure 6: Discretization of an existing MGB shaft

Each bearing is modeled with [6x6] matrixes (stiffness and damping) on the corresponding node of the shaft it carries. These two matrixes contain axial, radial and flexural stiffness and damping of the bearing.

External inertias (engine and load) are modeled on rotational DoF of input and output nodes in the global mass matrix.

Gear body is modeled as a disk with two [6x6] matrixes (mass and damping) on the node corresponding to the center of the gear. Mass matrix contains mass and inertias of the gear body. Damping matrix takes into account gyroscopic effects induced from the rotation speed of the gear. These matrixes are referenced in [13] [16].

We validated the model with two reference softwares, ROTORINSA and Code_Aster.

4.3. MODELING OF GEARS COUPLING

Elastic coupling of gears is realized with a specific stiffness element. It is a [12x12] stiffness matrix $K_{ms}(T,t)$ which couples DoF of the leading pinion with DoF of the leaded wheel using meshing stiffness defined in 3.2 and geometrical properties of gears. $K_{ms}(T,t)$ provides both kinematic coupling and instantaneous elastic coupling between centers of meshed gears. It is defined as follows [18]:

$$K_{ms}(T,t) = k(T,t) \cdot D^t \cdot D \qquad (7)$$

$D^t D$ is a [12x12] matrix which 'projects' $k(T,t)$ on nodes of centers of meshed gears and links their DoF. D is a [1x12] vector whose terms depend on both type and geometry of gears. D has often been defined in the local frame of meshed teeth in the case of gearboxes with only one cylindrical gear pair [12] [18]. We propose to extend this model to the case of transmissions with two or more cylindrical and/or spiral bevel gear pairs. To do this, DoF of D and all other matrixes described above have to be expressed in the global frame of the gearbox housing. Figure 7 and Figure 8 show cylindrical and spiral bevel geometrical parameters used to compute D in the global frame of gearbox housing.

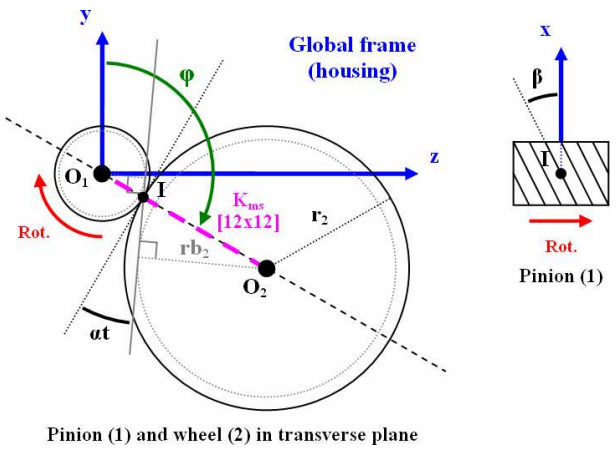

Figure 7: Cylindrical gears in the global frame

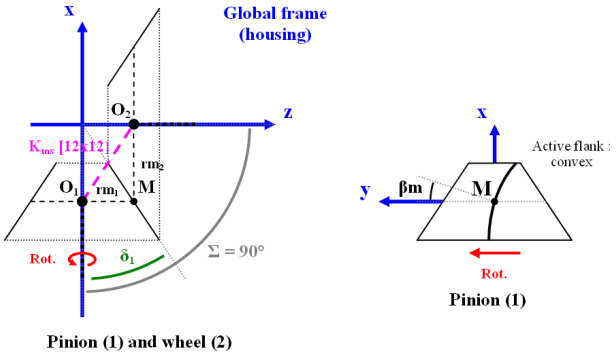

Figure 8: Spiral bevel gears in the global frame

Degrees of freedom of $K_{ms}(T,t)$ which couples nodes at gears centers (O_1 and O_2) in the global frame are the followings:

$$\{q_N\} = \{u_1 \quad v_1 \quad w_1 \quad \theta_{X1} \quad \theta_{Y1} \quad \theta_{Z1} \quad u_2 \quad v_2 \quad w_2 \quad \theta_{X2} \quad \theta_{Y2} \quad \theta_{Z2}\} \qquad (8)$$

D^t for cylindrical gears of Figure 7 in the global frame is the following:

$$D^t = \begin{bmatrix} -\cos(\alpha t)\cdot\tan(\beta) \\ -\cos(\alpha t)\cdot\sin(-\varphi)-\sin(\alpha t)\cdot\cos(-\varphi) \\ -\cos(\alpha t)\cdot\cos(-\varphi)+\sin(\alpha t)\cdot\sin(-\varphi) \\ r_1\cdot\cos(\alpha t) \\ -r_1\cdot\cos(\alpha t)\cdot\sin(-\varphi)\cdot\tan(\beta) \\ -r_1\cdot\cos(\alpha t)\cdot\cos(-\varphi)\cdot\tan(\beta) \\ \cos(\alpha t)\cdot\tan(\beta) \\ \cos(\alpha t)\cdot\sin(-\varphi)+\sin(\alpha t)\cdot\cos(-\varphi) \\ \cos(\alpha t)\cdot\cos(-\varphi)-\sin(\alpha t)\cdot\sin(-\varphi) \\ r_2\cdot\cos(\alpha t) \\ -r_2\cdot\cos(\alpha t)\cdot\sin(-\varphi)\cdot\tan(\beta) \\ -r_2\cdot\cos(\alpha t)\cdot\cos(-\varphi)\cdot\tan(\beta) \end{bmatrix} \quad (9)$$

r_i is the pitch radius of gear i
αt is the transverse pressure angle
β is the pitch helix angle
φ is the transverse angle between y axis (vertically in global frame) and center distance axis

D^t for spiral bevel gears isn't described in this paper. For this type of gears, D^t depends on the following geometrical properties (Figure 8):

rm_i (mean radius of gear i)
αn (pressure angle)
βm (mean spiral angle)
δ_1 (pitch angle of leading pinion)
Σ (shaft angle)

We validated matrix $K_{ms}(T,t)$ for cylindrical and spiral bevel gears with analytical exercises in order to verify static displacements and loads on centers of gears.

4.4. COMPUTATION OF DYNAMIC LOADS ON BEARINGS

The global transmission system is assembled with computed matrixes of shafts, bearings and gear pairs described above (4.2, 4.3). Then, the dynamic response is computed by solving equation (10):

$$\{\ddot{q}(t)\}[M]+\{\dot{q}(t)\}[C]+\{q(t)\}([K]+[G(t)])=\{F(t)\}+\{E(t)\} \quad (10)$$

In equation (10), $[K]$, $[M]$ and $[C]$ are three constant matrixes. These ones are the global stiffness, mass and damping matrixes of the modeled system. $[K]$ contains the mean value of $K_{ms}(T,t)$.

Excitation matrixes of equation (10) are $[G(t)]$, $[F(t)]$ and $[E(t)]$. $[G(t)]$ is a stiffness matrix introducing the mechanical excitations induced from time variations of $K_{ms}(T,t)$. $\{F(t)\}$ is the vector of external loads induced from the operating torque T. In the case of steady torque (without oscillation), $\{F(t)\}$ becomes $\{F\}$ constant. $\{F(t)\}$ is applied to input and output nodes of the system. $\{E(t)\}$ is the vector of internal loads induced from the product of variations of STE by variations of meshing stiffness. $\{E(t)\}$ is applied at gears centers.

$\{q(t)\}$ is the solution giving displacements of all DoF of the system. Using these displacements and stiffnesses of bearings, we compute dynamic loads on these later:

$$\{F_{i\_B}(t)\}=k_{i\_B}\cdot\{q_{i\_B}(t)\} \quad (11)$$

$\{F_{i\_B}(t)\}$ is the dynamic load on bearing B, corresponding to DoF i in the global frame of gearbox housing. k_{i_B} is the stiffness of bearing B corresponding to DoF i.

In order to be analyzed, magnitude and phase spectra of dynamic loads on bearings have to be computed, so as to be used as inputs in noise radiation computation with FEM solver (step 3 of the methodology Figure 3).

5. EXEMPLE OF APPLICATION

An example of result is proposed here to compute longitudinal dynamic loads on bearing B5 (Figure 9) for two cases of meshing stiffnesses. In this application, meshing stiffnesses are synthetic signals but, as we told in 3, they could have been computed using EC tools for realistic gears. The system is representative of a MGB input. It is composed of 3 shafts, 8 bearings and 2 gear pairs (spur cylindrical and spiral bevel). It is modeled with elements described in 4. Operating conditions (speed and torque) of the both cases are similar.

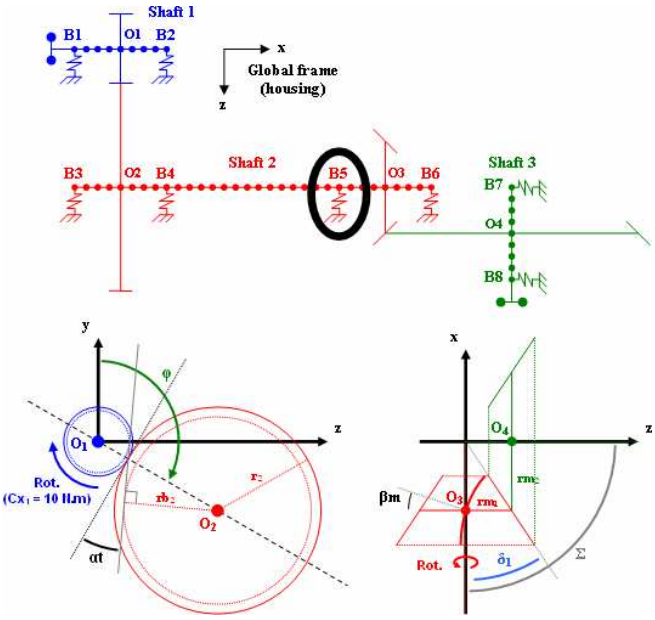

Figure 9: Transmission system with two gear pairs

Meshing stiffnesses of case 1 simulate optimal gears. In this case, meshing stiffnesses don't fluctuate much and are perfectly continuous. The simple model chosen here is pure sinus at gear mesh frequencies (Figure 10):

Spur cylindrical gear pair:

$$k_1(T,t)=k\cdot(1+0{,}1\cdot\sin(2\pi\cdot fe_1\cdot t))$$

Spiral bevel gear pair:

$$k_2(T,t)=k\cdot(1+0{,}1\cdot\sin(2\pi\cdot fe_2\cdot t))$$

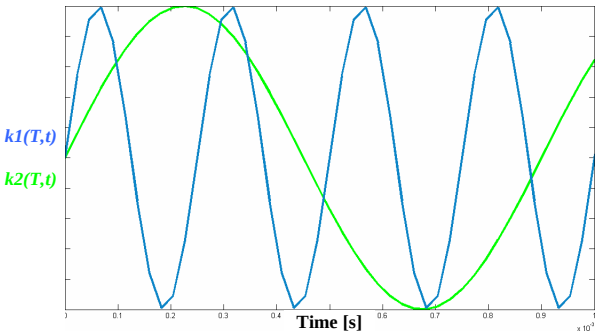

Figure 10: Meshing stiffnesses of case 1

Meshing stiffnesses of case 2 simulate realistic gears. In this case, meshing stiffnesses are deteriorated regarding case 1. They are modeled with sums of sinus harmonics of gear mesh frequencies and variations are doubled for bevel gear pair (Figure 11):

Spur cylindrical gear pair:

$$k_1(T,t) = k \cdot \left(1 + 0{,}1 \cdot \sum_{n=1,3,5} \frac{\sin(2\pi \cdot n \cdot fe_1 \cdot t)}{n}\right)$$

Spiral bevel gear pair:

$$k_2(T,t) = k \cdot \left(1 + 0{,}2 \cdot \sum_{n=1,3,5} \frac{\sin(2\pi \cdot n \cdot fe_2 \cdot t)}{n}\right)$$

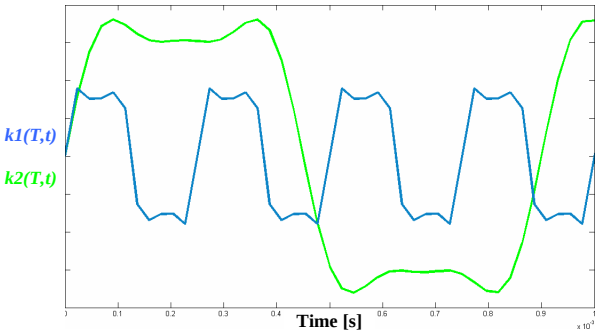

Figure 11: Meshing stiffness of case 2

fe_1 and fe_2 are the fundamental gear mesh frequencies of gear pairs.

Dynamic loads computed on bearing B5 in the global frame are:

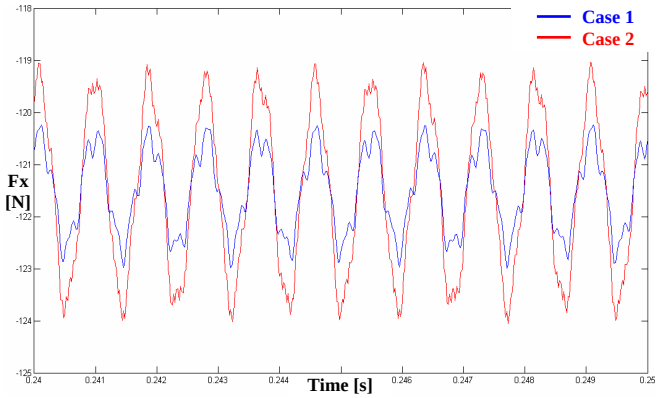

Figure 12: Dynamic load Fx on bearing B5 (cases 1 & 2)

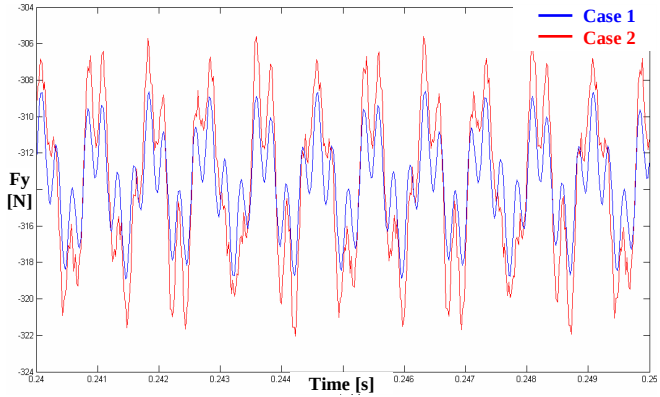

Figure 13: Dynamic load Fy on bearing B5 (cases 1 & 2)

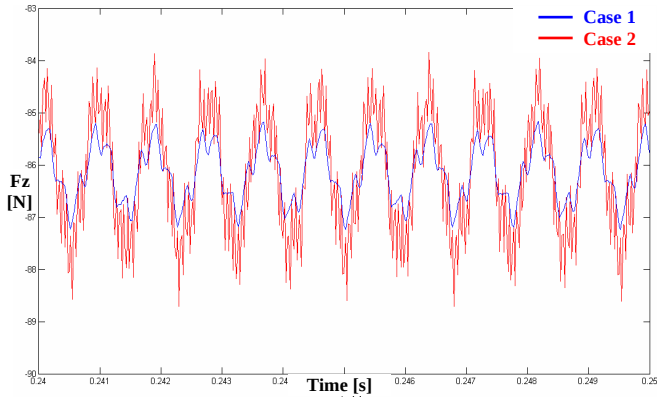

Figure 14: Dynamic load Fz on bearing B5 (cases 1 & 2)

Magnitude spectra of dynamic loads on bearing B5 are:

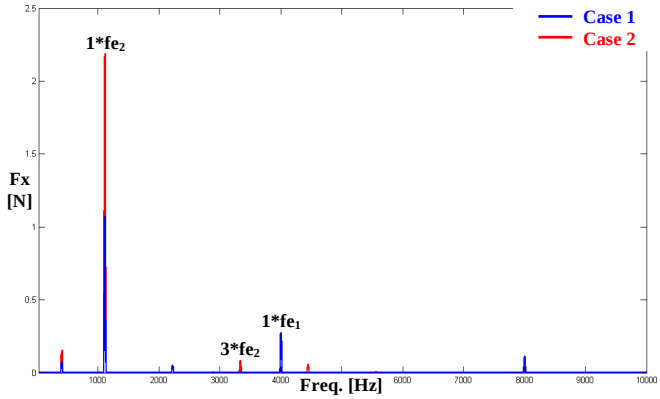

Figure 15: Magnitude spectrum of Fx on bearing B5

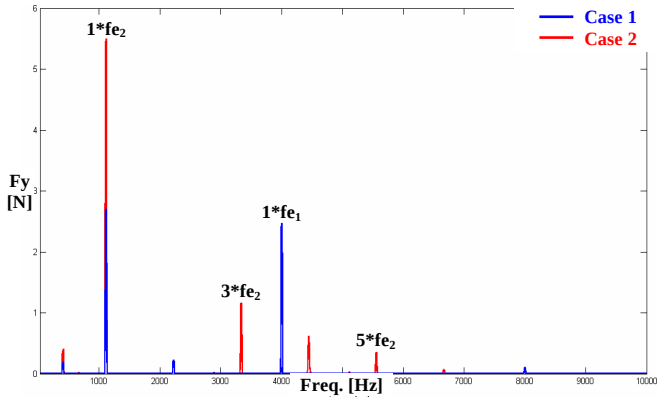

Figure 16: Magnitude spectrum of Fy on bearing B5

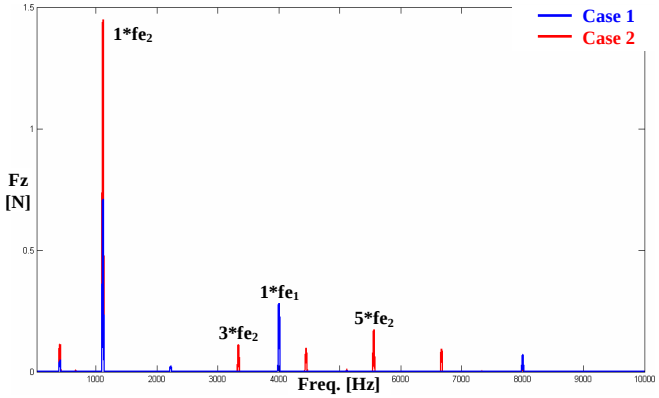

Figure 17: Magnitude spectrum of Fz on bearing B5

We observe expected results: level and frequency of dynamic loads on bearings are particularly sensitive to gear mesh excitations, static transmission error and meshing stiffness. Indeed, dynamic loads levels in case 1 ('optimal gears') are lower than the ones of case 2 ('realistic gears'). In particular, level of $1*fe_2$ in case 2 is twice the level of $1*fe_2$ in case 1. This is due to meshing stiffness variations that are doubled for the bevel gear pair in case 2. Moreover, spectra contents are richer in case 2 than in case 1. This is also due to differences of meshing stiffness signal between the two cases.

In this application, meshing stiffnesses of gear pairs were simulated with synthesis signals but methodology is similar in the case of realistic signals computed with EC tools described in 3. Thus, using our model, we are able to compute dynamic loads on bearings of realistic helicopter MGB. These results are interesting for several reasons. Firstly, it is now possible to better understand vibro-acoustic behavior of gearboxes. Secondly, modifications of geometrical and material properties can be simulated to study their effects on operating gearboxes. At last, this modeling will now be improved and used during development phases of Eurocopter MGB in order to design quieter gears to improve acoustic comfort in helicopter cabins.

6. CONCLUSION

In this paper, we described the current EC/LRMA developments regarding the modeling of gearboxes noise. We proposed a methodology to compute main gearboxes noise in helicopter cabins based on several steps.

The first step computes static transmission error (STE) and meshing stiffness of gear pairs under quasi-static load. They describe the elastic coupling between meshed gears and are the dominant mechanical excitation sources due to gear mesh. We compute those using either analytical tool or EC tools.

The second step consists in computing drive train dynamic response to STE and meshing stiffness excitations. In this step, all components of gearbox are modeled except for housing. The target is to compute dynamic loads on bearings which are the vibratory excitations generating housing noise radiation. To do this, we developed a stand-alone MATLAB program using a finite element matrixial method. This program is able to model and solve complex problems with two or more cylindrical and/or spiral bevel gear pairs. It also takes into account shear effects and gyroscopic effects of components. Output data are all dynamic loads spectra computed on bearings.

Third step was introduced without result. The target is to compute overall acoustic and vibration behavior of the full system including housing. This work will be tackled during the coming months using a commercial tool.

At last, using our current model, we are able to compute and better understand vibro-acoustic behavior of operating gearboxes. We will now use it during development phases of EC MGB in order to design quieter gears to improve acoustic comfort in helicopter cabins.

BIBLIOGRAPHY

[1] **J. CAILLET**, Diagnostic et modélisation du bruit et des chemins de bruits en cabine d'hélicoptère, 218p. (Eurocopter 2006)

[2] **D. R. HOUSER**, Gear noise. State of the art, Proceedings of Inter-Noise 1988, p. 601-606 (1988)

[3] **W. D. MARK**, Gear noise origins, Proceedings of AGARD conference, p. 30.1-30.14 (1985)

[4] **A. M. THOMPSON**, Origins of gear noise, Proceedings of the 2nd world congress on gearing, p. 1809-1817 (1977)

[5] **D. B. WELBOURN**, Fundamental knowledge of gear noise - A survey, Proceedings of conference on 'Noise and Vibrations of Engines and Transmissions', p. 9-14 (1979)

[6] **P. DUCRET**, Prédiction du bruit rayonné par les carters des transmissions à engrenages, 160p. (1997)

[7] **D. REMOND, P. VELEX, J. SABOT**, Comportement dynamique et acoustique des transmissions par engrenages – Synthèse bibliographique, 189p. (1993)

[8] **J. PERRET-LIAUDET**, Quelques aspects sur la prédiction du comportement vibroacoustique des engrenages, Journée SFA, 7p. (2002)

[9] **N. DRIOT**, Etude de la dispersion vibroacoustique des transmissions par engrenages, 165p. (2002)

[10] **R. G. MUNRO**, The D. C. component of gear transmission error, Proceedings of the 5th ASME International Power Transmission and Gearing Conference, p. 467-470 (1989)

[11] **Y. ICARD**, Engrenage spiro-conique : Modélisation sous charge appliquée au domaine aéronautique, 264p. (Eurocopter 2005)

[12] **C. BARD**, Modélisation du comportement dynamique des transmissions par engrenages, 296p. (1992)

[13] **M. TORKHANI**, Code_Aster - Matrice gyroscopique des poutres et disques [R5.05.07], 10p. (2009)

[14] **J.-L. FLEJOU**, Code_Aster - Eléments « exacts » de poutres (droites et courbes) [R3.08.01], 69p. (2009)

[15] **J.-F. IMBERT**, Analyse des structures par éléments finis, 506p. (1995)

[16] **M. LALANNE, G. FERRARIS**, Rotordynamics – Prediction in Engineering (seconde édition), 254p. (1998)

[17] **J. S. PRZEMIENIECKI**, Theory of Matrix Structural Analysis, 467p. (1968)

[18] **E. RIGAUD**, Interactions dynamiques entre denture, lignes d'arbres, roulements et carter dans les transmissions par engrenages, 177p. (1998)